



## ORIGINAL ARTICLE

# Trigothyoid N inhibits tumor proliferation and migration by targeting mitochondria and the STAT3/FAK pathway



Ying Li <sup>a</sup>, Yuhui Liu <sup>a</sup>, Yeling Li <sup>a</sup>, Feng Liu <sup>a</sup>, Yinan Zhao <sup>a</sup>, Jing Xu <sup>a,\*</sup>,  
Yuanqiang Guo <sup>a,b,\*</sup>

<sup>a</sup> State Key Laboratory of Medicinal Chemical Biology, College of Pharmacy, and Tianjin Key Laboratory of Molecular Drug Research, Nankai University, Tianjin 300350, People's Republic of China

<sup>b</sup> Key Laboratory of Tropical Medicinal Resource Chemistry of Ministry of Education, Hainan Normal University, Haikou, Hainan 571158, People's Republic of China

Received 25 June 2022; accepted 22 April 2023

Available online 26 April 2023

## KEYWORDS

Natural diterpenoid;  
Anti-tumor activity;  
Zebrafish xenograft model;  
Mitochondria;  
STAT3;  
FAK

**Abstract** Natural products are one of the essential sources of innovative drugs. Trigothyoid N, a natural daphnane diterpenoid obtained from *Trigonostemon thyrsoides*, possessed the strong ability to inhibit the proliferation of A549 cells. Besides interrupting the cell cycle, the mechanism examination revealed that trigothyoid N can inhibit tumor proliferation and migration by targeting mitochondria, regulating the STAT3/FAK signal pathway, and suppressing angiogenesis. In addition to the possible mechanism, *in vivo* antitumor experiments were performed to explore the potential of trigothyoid N for treating non-small cell lung cancer (NSCLC). Collectively, these findings supported the great potential of trigothyoid N as a hopeful therapeutic agent against NSCLC.

© 2023 The Author(s). Published by Elsevier B.V. on behalf of King Saud University. This is an open access article under the CC BY license (<http://creativecommons.org/licenses/by/4.0/>).

## 1. Introduction

Globally, cancer ranks first among the causes of death (Sung et al., 2021). In 2020, the number of new cancer cases increased to 19.3 million, while the number of cancer deaths rose to 10 million. The incidence rate and death data related to cancer suggest that most death

cases are attributed primarily to cancer all over the world. Lung cancer is the common cancer after female breast cancer accounting for 11.4% of the total cases, most of which are categorized as non-small cell lung cancer (NSCLC) with about 1.8 million deaths per year (Sung et al., 2021). Among numerous treatment options including surgery, radiotherapy, and immunotherapy, chemotherapy is the most common treatment for NSCLC (Ferlay et al., 2021; Dai et al., 2021; Courdavault et al., 2020). However, in addition to the drug resistance decreasing the treatment efficiency, long-term chemotherapy often leads to serious side effects, which are a crucial problem that must be faced. Therefore, developing novel and efficient drugs with high efficacy and fewer side effects for the treatment of NSCLC is urgently required (Sung et al., 2021; Ferlay et al., 2021).

\* Corresponding authors at: State Key Laboratory of Medicinal Chemical Biology, College of Pharmacy, and Tianjin Key Laboratory of Molecular Drug Research, Nankai University, Tianjin 300350, People's Republic of China (Y. Guo).

E-mail addresses: [xujing611@nankai.edu.cn](mailto:xujing611@nankai.edu.cn) (J. Xu), [victgyq@nankai.edu.cn](mailto:victgyq@nankai.edu.cn) (Y. Guo).

Nature has created many compounds with a diversity of structure and biological activity, which are also called natural products. As a source of new drugs, natural products have been crucial to the development of innovative drugs, and most of the drugs currently used come from natural products or their imitations. For cancer treatment, there have been some well-known examples from natural products, such as paclitaxel and camptothecin. In our search for bioactive natural products from medicinal plants, the genus *Trigonostemon* plants, belonging to the *Euphorbiaceae* family, evoked our attention, because some *Trigonostemon* plants have been utilized historically as folk remedies for a variety of diseases in China and Thailand (Cheng et al., 2013). The main ingredients have been investigated and reported to be diterpenoids and alkaloids, which displayed a range of biological effects including cytotoxic, anti-leukemic, insecticidal, and anti-bacterial properties (Cheng et al., 2013; Liu et al., 2018; Liu et al., 2017). Our chemical isolation led to the obtainment of a natural daphnane-type diterpenoid, trigothysoid N, from *Trigonostemon thyrsoideus*, which was reported to possess potent anti-HIV-1 activity previously (Liu et al., 2017). Nevertheless, as far as we know, there have been no reports on the antitumor activity, especially *in vivo* antitumor activity, and the related mechanism of this natural daphnane-type diterpenoid, trigothysoid N. In our subsequent biological screening, trigothysoid N showed strong antitumor activity toward A549, HepG2, and HeLa cells and possessed the most inhibitory property against A549 cells.

Based on the *in vitro* activity assay, this study attempts to clarify the possible mechanism of suppressing tumor migration and proliferation from the aspects of cell apoptosis, cell cycle, reactive oxygen species (ROS) production, mitochondrial membrane potential (MMP) changes, cell migration, and tumor angiogenesis. In view of the intrinsic properties of the tumor, the expression of some key proteins related to the tumor proliferation and migration in the signal transducer and activator of transcription 3 (STAT3) and focal adhesion kinase (FAK) pathways affected by trigothysoid N was investigated. Furthermore, the application prospect of the natural diterpenoid trigothysoid N in cancer treatment was explored using the zebrafish tumor model.

## 2. Materials and methods

### 2.1. Materials and cell culture

Fetal bovine serum (FBS, BI, Israel) and Dulbecco's modified Eagle's medium (DMEM) were obtained from Lab Biotech Co. Ltd. (Shandong, China). MTT was purchased from Bio-Froxx (Guangzhou, China) and DMSO was purchased from Solarbio Co. Ltd. (Beijing, China). Cell tracker CM-DiI was obtained from Yeasen Biotechnology Co. Ltd. (Shanghai, China). Annexin V-FITC apoptosis detection kit, cell cycle and apoptosis kit, MMP assay kit with JC-1, reactive oxygen species assay kit, BCA protein assay kit were obtained from Beyotime Biotechnology Co. Ltd. (Shanghai, China). Rabbit monoclonal antibodies to Bax (Cat# 14796), Bcl-2 (Cat# 4223), STAT3 (Cat# 9139), phospho-STAT3 (Tyr 705) (Cat# 9145), FAK (Cat# 3285), phospho-FAK (Tyr 397) (Cat# 8556), matrix metalloproteinase-2 (Cat# 87809), and  $\beta$ -actin (Cat# 4970) were all purchased from Cell Signaling Technology (Danvers, MA, USA). All chemicals and reagents are analytical grade and ready for direct use. Human lung adenocarcinoma cell line (A549), human hepatoma cell line (HepG2), and human cervical cancer cell line (HeLa) were obtained from Shanghai Institutes for Biological Sciences, Chinese Academy of Sciences (Shanghai, China). All cells were maintained in DMEM containing 10% (v/v) FBS and 100

U/mL antibiotics (penicillin/streptomycin) at 37 °C in a humidified atmosphere of 5%CO<sub>2</sub>. Adult AB and transgenic zebrafish were acquired from Shanghai Feixi Biotechnology Co., Ltd. (Shanghai, China).

### 2.2. Anti-proliferation activity assay

The MTT assay was used to determine the cytotoxic activity of trigothysoid N toward A549, HepG2, and HeLa cell lines (Li et al., 2021). The detailed method is shown in the [Supplementary data](#).

### 2.3. Apoptosis analysis by flow cytometry

The effects of trigothysoid N on A549 cell apoptosis were assessed by flow cytometry using Annexin V-FITC apoptosis detection kit (Beyotime, Shanghai, China) (Zhou et al., 2021; Bao et al., 2021). The specific procedures are described in the [Supplementary data](#).

### 2.4. Cell cycle analysis

The role of trigothysoid N in cell cycle distribution was monitored using flow cytometric analysis (Yin et al., 2022; Zhang et al., 2021c). The detailed procedure is supplemented in the [Supplementary data](#).

### 2.5. MMP evaluation

MMP was detected by the MMP dye JC-1 (Beyotime, Shanghai, China) (Kim et al., 2016; Fan et al., 2020). The details for this experiment are described in the [Supplementary data](#).

### 2.6. Measurement of ROS

The levels of intracellular ROS were detected using the ROS assay kit (Beyotime, Shanghai, China) (Zhao et al., 2022; Ye et al., 2017). The details of this experiment are described in the [Supplementary data](#).

### 2.7. Wound-scratch assay

The migration of A549 cells inhibited by trigothysoid N was measured by wound-healing assay (Lin et al., 2022). The experimental details are provided in the [Supplementary data](#).

### 2.8. Western blotting analysis

Western blotting analysis was carried out to quantify the levels of protein expression (Wu et al., 2020a). The specific procedures for Western blotting analysis are provided in the [Supplementary data](#).

### 2.9. Zebrafish husbandry and maintenance

Adult zebrafish were maintained and fed according to standard procedures (Shi et al., 2022). The details are shown in the [Supplementary data](#).

### 2.10. Antiangiogenic assay using transgenic zebrafish

The inhibition of trigothyroid N toward angiogenesis was assessed using transgenic zebrafish *Tg (fli1:EGFP)* embryos (Zhang, et al., 2021b; Zhou et al., 2022). The detailed method for this experiment is shown in the [Supplementary data](#).

### 2.11. In vivo antitumor assay using zebrafish tumor xenografts

A zebrafish xenograft model was constructed to analyze the impact of trigothyroid N on tumor cell proliferation and metastasis (Liang et al., 2020; Zhang et al., 2021a). The specific procedures are described in the [Supplementary data](#).

### 2.12. Statistical analysis

GraphPad Prism 7.0 software was used to analyze the experimental data. All data are presented as mean  $\pm$  SD. Significant differences among different groups were compared by one-way ANOVA. Probabilities (P) less than 0.05 meant a statistically significant difference. All of the experiments were repeated three times.

## 3. Results

### 3.1. Trigothyroid N inhibited tumor cell proliferation *in vitro*

To further explore whether trigothyroid N had antitumor effects *in vitro*, an MTT assay was performed to examine the anti-proliferation activity of trigothyroid N against three types of human cancer cells (A549, HepG2, and HeLa cells). As shown in [Fig. 1A–C](#), trigothyroid N suppressed tumor cell

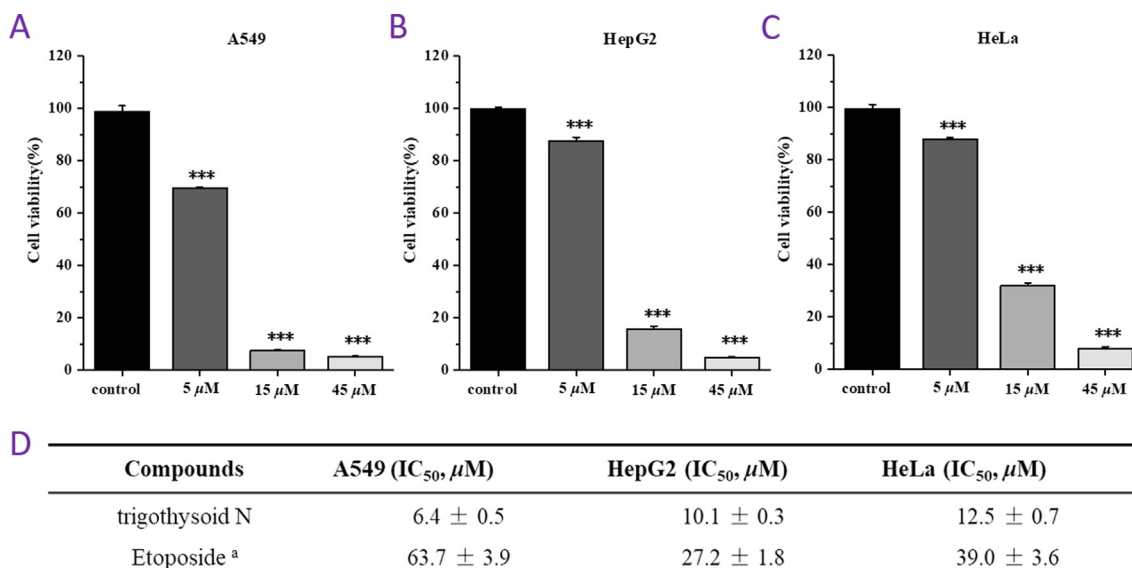
growth in a dose-dependent manner according to the MTT experimental results, and the IC<sub>50</sub> values for three cell lines were 6.4 (A549 cells), 10.1 (HepG2 cells), and 12.5  $\mu$ M (HeLa cells), respectively ([Fig. 1D](#)). According to the IC<sub>50</sub> values of trigothyroid N and the positive control etoposide, trigothyroid N showed strong anti-proliferation effects against the selected tumor cell lines.

### 3.2. Apoptotic effects of trigothyroid N on A549 cells

Trigothyroid N showed promising antitumor activity against three tumor cells and had the most inhibitory effects toward A549 cells. To explore whether the anti-proliferation activity of trigothyroid N against A549 cells was related to cell apoptosis, an Annexin V-FITC/PI assay was carried out by flow cytometry (Ye et al., 2016). As depicted in [Fig. 2](#), a dose-dependent increase in early and late apoptotic cells was observed. After exposure to various concentrations (5.0, 10.0, and 20.0  $\mu$ M) of trigothyroid N for 48 h, the apoptotic cell percentages increased from 9.9% (control) to 12.6% (5.0  $\mu$ M), 15.4% (10.0  $\mu$ M), and 59.0% (20.0  $\mu$ M). According to these findings, trigothyroid N caused the apoptosis of A549 cells in a dose-dependent manner.

### 3.3. Effects of trigothyroid N on cell cycle

The apoptosis experiments showed trigothyroid N to have the ability of inducing the apoptosis of A549 cells. Cell apoptosis is closely coupled with cell cycle progression, which is caused by cell cycle termination and disruption (Yao et al., 2020). To understand whether the cell cycle was affected by trigothyroid N, the cell cycle distribution of A549 cells was examined using flow cytometry. As shown in [Fig. 3A](#), after



<sup>a</sup> Etoposide was used as a positive control. All results are expressed as the mean  $\pm$  SD.

**Fig. 1** Anti-proliferative effects of trigothyroid N on three cell lines. Cytotoxicities of trigothyroid N against three human cancer cell lines were tested. A549 (A), HepG2 (B) and HeLa (C) cells were treated with trigothyroid N (5, 15, and 45  $\mu$ M) for 48 h. Cell viability was examined using the MTT assay. (D) List of IC<sub>50</sub> values of trigothyroid N on several cancer cell lines. DMSO was used as a negative control. The results are presented as mean  $\pm$  SD. n = 3, \*\*\*P < 0.001 versus control group.

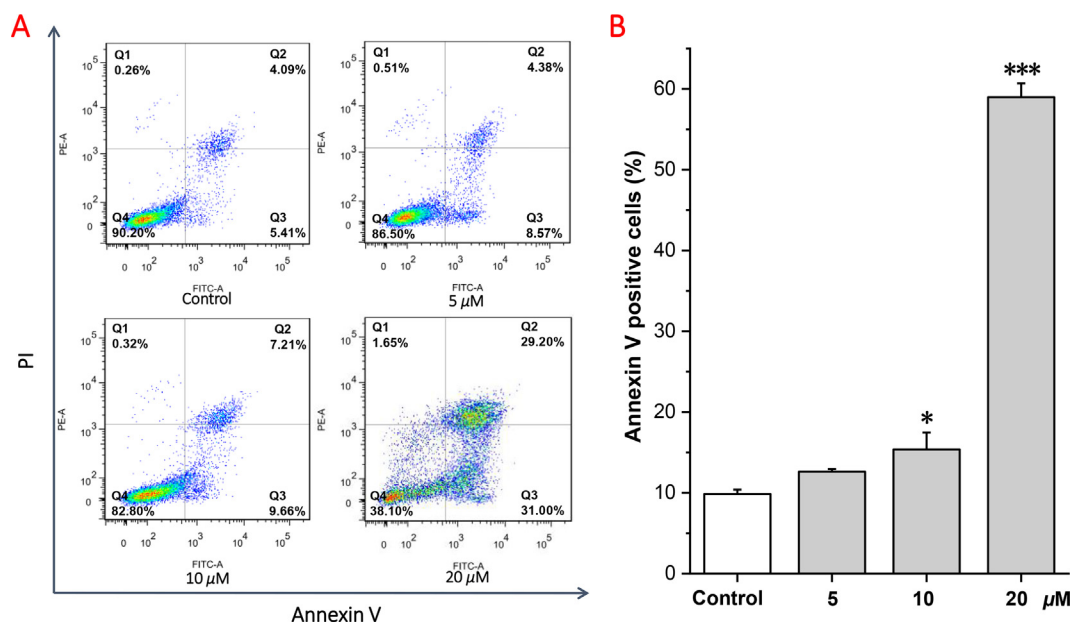


**Fig. 2** Apoptosis effects of A549 cells induced by trigothysoid N. A549 cells were treated with different concentrations (5, 10, and 20 μM) of trigothysoid N for 48 h. DMSO was used as a negative control. Then the cells were harvested, stained with Annexin V and propidium iodide (PI), and subsequently analyzed by flow cytometry. (A) Flow cytometric analysis of A549 cells treated with different concentrations of trigothysoid N. (B) Histogram of apoptotic cells at 48 h with the treatment of trigothysoid N. Data from three separate experiments are expressed as mean ± SD.  $n = 3$ , \* $P < 0.05$ , \*\*\* $P < 0.001$  versus control group.

treatment with trigothysoid N for 48 h, A549 cells were clearly arrested at the G0/G1 phase, and the arrest effects were dose-dependent. According to the quantification results as illustrated in Fig. 3B, when the concentration of trigothysoid N increased from 5.0 μM to 20.0 μM, the proportions of cells in G1 phase increased from 64.1% (control) to 79.0% (5.0 μM), 86.6% (10.0 μM), and 89.0% (20.0 μM), while the percentages in S and G2 phases decreased. The cell cycle experiments revealed that trigothysoid N can arrest the cell cycle at G0/G1 phase.

#### 3.4. Trigothysoid N induced the loss of MMP

The apoptosis of tumor cells is usually coupled with abnormal changes in MMP. To confirm that the alteration of MMP was involved in the induction of apoptosis, the fluorescent mitochondrial probe JC-1 was used to detect MMP with flow cytometry (Li et al., 2015). As shown in Fig. 4B and C, a large portion of the red fluorescence was changed to green (Fig. 4A). When the dose of trigothysoid N increased, the JC-1 polymer and the JC-1 polymer/monomer ratio both dramatically dropped. Collectively, the MMP detection implied that trigothysoid N can induce MMP depolarization to stimulate A549 cell apoptosis.

#### 3.5. Trigothysoid N induced ROS generation in A549 cells

In addition to the abnormal changes in MMP, cell apoptosis is often accompanied by a large increase of ROS production in mitochondria. It has been reported that ROS is crucial for many biochemical processes and physiological reactions, such as cell proliferation and apoptosis. Excessive ROS in mitochondria usually prompts cell apoptosis (Zhang et al., 2015). To confirm whether the apoptosis of A549 cells was coupled

with the ROS increase in mitochondria, the ROS levels in trigothysoid N-treated A549 cells were quantified. As illustrated in Fig. 4D, when A549 cells were treated with trigothysoid N, the ROS levels were elevated concurrently. According to the statistical results, with the concentration increase of trigothysoid N, the ROS levels rose by 4-fold (6.25 μM), 10-fold (12.5 μM), and 23-fold (25.0 μM) in A549 cells when compared with the control group (Fig. 4E). The ROS detection implicated that the diterpenoid trigothysoid N stimulated ROS generation to prompt the apoptosis of A549 cells.

#### 3.6. Trigothysoid N induced apoptosis by mitochondria-dependent signaling

Apoptosis induced by ROS often leads to alterations in the pro-apoptosis protein expression in ROS dependent pathway, which leads to apoptosis. Thus, Western blotting experiments were carried out to investigate the related protein expression of mitochondrial-dependent apoptosis pathway (Kim et al., 2016). As shown in Fig. 5A and 5C, the levels of Bax, a pro-apoptotic protein, were upregulated with the concentration increase of trigothysoid N. Additionally, the expression of Bcl-2, an anti-apoptotic protein, was significantly downregulated. The changes in protein expression, together with the aforementioned MMP and ROS detection, suggested that trigothysoid N could trigger ROS and alter MMP to stimulate A549 cell apoptosis.

#### 3.7. Trigothysoid N regulated STAT3 signal pathway

Accumulating studies have reported that tumor proliferation is regulated by STAT3 and downstream proteins (Chen et al., 2018). To clarify whether trigothysoid N affected the STAT3/p-STAT3-related signal pathway, the protein expres-

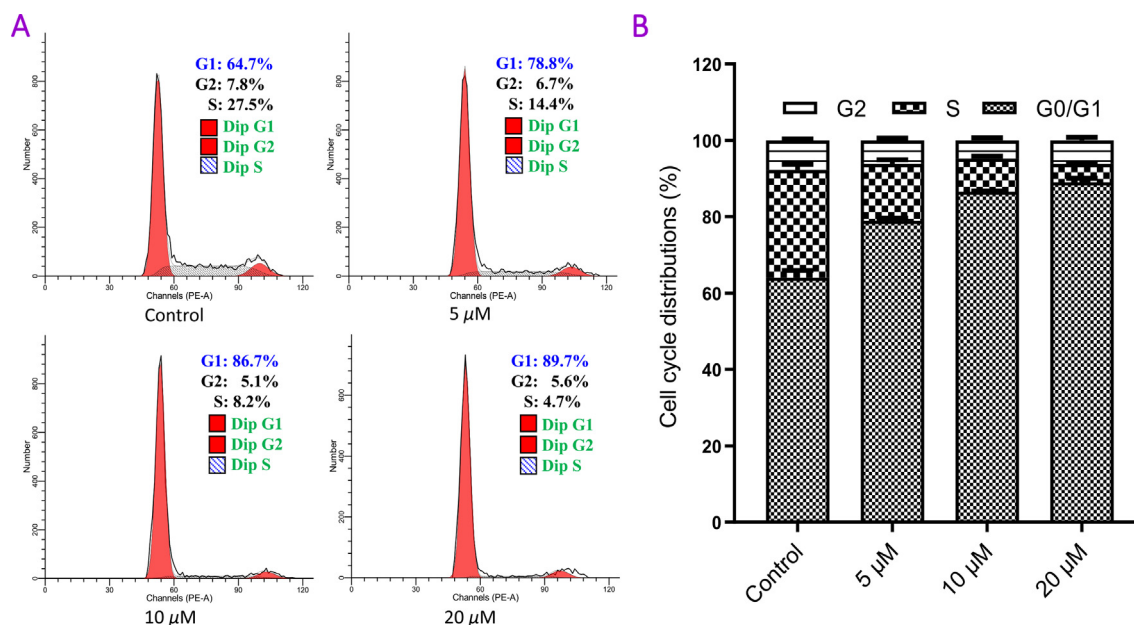


**Fig. 3** Effects of trigothyroid N on A549 cell cycle arrest. A549 cells were treated with different concentrations (5, 10, and 20  $\mu$ M) of trigothyroid N for 48 h. DMSO was used as a negative control. (A) The cells were harvested and stained with propidium iodide (PI), and the cell cycle distribution was analyzed using flow cytometry. (B) Histogram of cell cycle phases distribution. Data from three separate experiments are expressed as mean  $\pm$  SD.

sion of STAT3 and p-STAT3 was detected by Western blotting experiments. As shown in Fig. 5E–F, trigothyroid N was shown to suppress p-STAT3 (Tyr705) in a dose-dependent way, in which the expression of p-STAT3 were 0.69- (5.0  $\mu$ M), 0.37- (10.0  $\mu$ M), and 0.05- (20.0  $\mu$ M) fold of the control. However, after being treated with trigothyroid N, the protein levels of STAT3 were not changed. In addition to the change of p-STAT3 (Tyr705) protein expression, the downstream proteins Bcl-2 (an anti-apoptotic protein) and Bax (a pro-apoptosis protein) of the STAT3 signal pathway were significantly downregulated and upregulated, respectively. All of the experimental results pointed out that trigothyroid N regulated the phosphorylation of STAT3 protein to promote A549 cell apoptosis.

### 3.8. Trigothyroid N inhibited A549 cell metastasis via regulating FAK signal pathway

Migration is another important characteristic of tumors. To assess the inhibitory potential of trigothyroid N against A549 cell migration, a wound-healing test was conducted (Fan et al., 2020; Rocha-Brito et al., 2020). As shown in Fig. 6A–B, the cell gap closure was inhibited significantly after treatment with trigothyroid N, and the migration rates of A549 cells were 75.3% (control), 64.8% (5.0  $\mu$ M), 34.6% (10.0  $\mu$ M) and 10.4% (20.0  $\mu$ M), respectively, according to the wound-healing results.

Tumor migration is regulated by numerous genes and proteins, of which focal adhesion kinase (FAK) and the downstream proteins are considered to be crucial and participate in regulation. The following experiments were thus designed to detect the expression of FAK, p-FAK, and the downstream-related proteins. According to the Western blot-

ting results, trigothyroid N had no effects on the expression of FAK (Fig. 6E), but affected the expression of the phosphorylation of FAK and matrix metalloproteinase-2, which decreased significantly in a dose-dependent manner. The changes of p-FAK expression and the downstream protein matrix metalloproteinase-2 implied that trigothyroid N exerted antimetastatic activity in A549 cells by regulating FAK pathway.

### 3.9. Antiangiogenic activity of trigothyroid N using a transgenic zebrafish model

As reported in numerous studies, angiogenesis is crucial for the development and progression of tumors, providing and transporting essential nutrients for tumor proliferation (Yu et al., 2016). To reveal whether trigothyroid N affected angiogenesis, a transgenic zebrafish (*flil:EGFP*) model was applied, in which the vessels presented green fluorescence and were easy to observe and quantify (Wang et al., 2023). As shown in Fig. 7, the vessels in the control-group embryos developed normally, while the intersegmental blood vessels (ISVs) and dorsal longitudinal anastomotic vessels (DLAVs) were disrupted after being treated with trigothyroid N. According to quantitative analysis by ImageJ, the average length of ISVs in the control group was 2530.8  $\mu$ m, and the length of ISVs in the group treated by trigothyroid N decreased dose-dependently, which were 2086.6  $\mu$ m (0.025  $\mu$ M of trigothyroid N), 2066.5  $\mu$ m (0.05  $\mu$ M of trigothyroid N), and 448.5  $\mu$ m (0.1  $\mu$ M of trigothyroid N), respectively. The transgenic zebrafish experiments indicated that trigothyroid N inhibited angiogenesis and was potential to become an antiangiogenic agent for NSCLC.

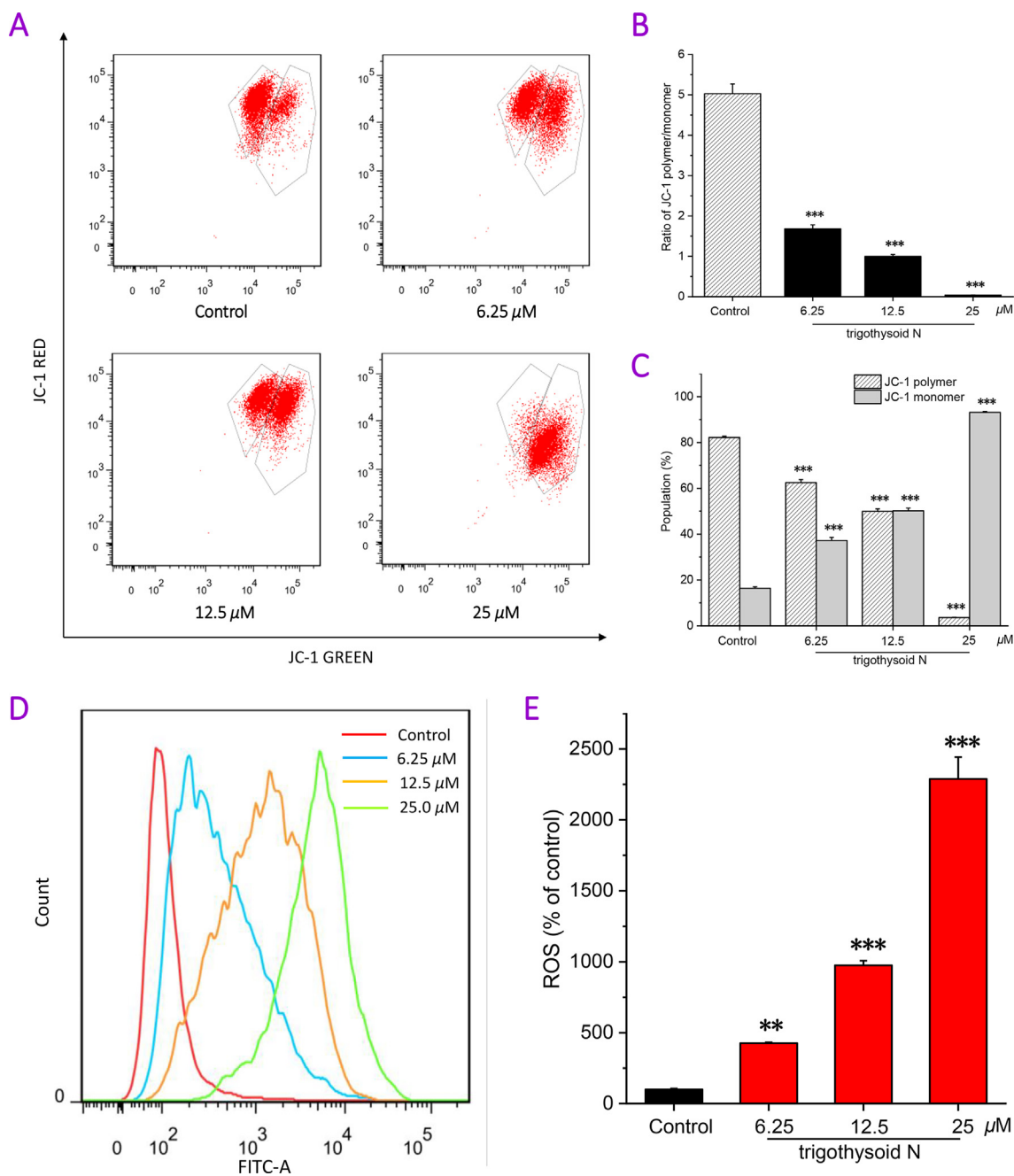


**Fig. 4** Trigothysoid N induced the loss of MMP and increased cellular ROS production. (A) A549 cells were incubated with different concentrations of trigothysoid N (6.25, 12.5, and 25 μM) for 48 h and the change of MMP was determined using JC-1 dye with flow cytometry analysis. (B) The ratio of polymer to monomer intensity and (C) the percentage of polymer and monomer were analyzed to show the quantitative change of MMP. (D) Trigothysoid N induced the generation of intracellular ROS. Cells were pretreated with 6.25, 12.5, and 25 μM trigothysoid N for 48 h before DCFH-DA was employed to detect the change of ROS via flow cytometry. (E) Quantification of the mean fluorescence intensity representing ROS production from three independent experiments. Data from three separate experiments are expressed as mean ± SD. n = 3, \*\**P* < 0.01, \*\*\**P* < 0.001 versus control group.

### 3.10. *In vivo* antitumor activity of trigothysoid N using a zebrafish model

The cellular and transgenic zebrafish experiments have demonstrated that trigothysoid N can suppress the proliferation and migration of A549 cells and block angiogenesis. These results prompted us to further examine the *in vivo* antiproliferative

and antimetastatic effects of trigothysoid N, which may reveal the potential to become an antitumor agent against NSCLC. By microinjecting stained A549 cells into zebrafish embryos, the zebrafish xenograft model was established. In this model, the tumor proliferation and metastasis were reflected by the fluorescent density and foci in zebrafish (Ye et al., 2017; Wang et al., 2022a, 2022b). As presented in Fig. 8, in contrast

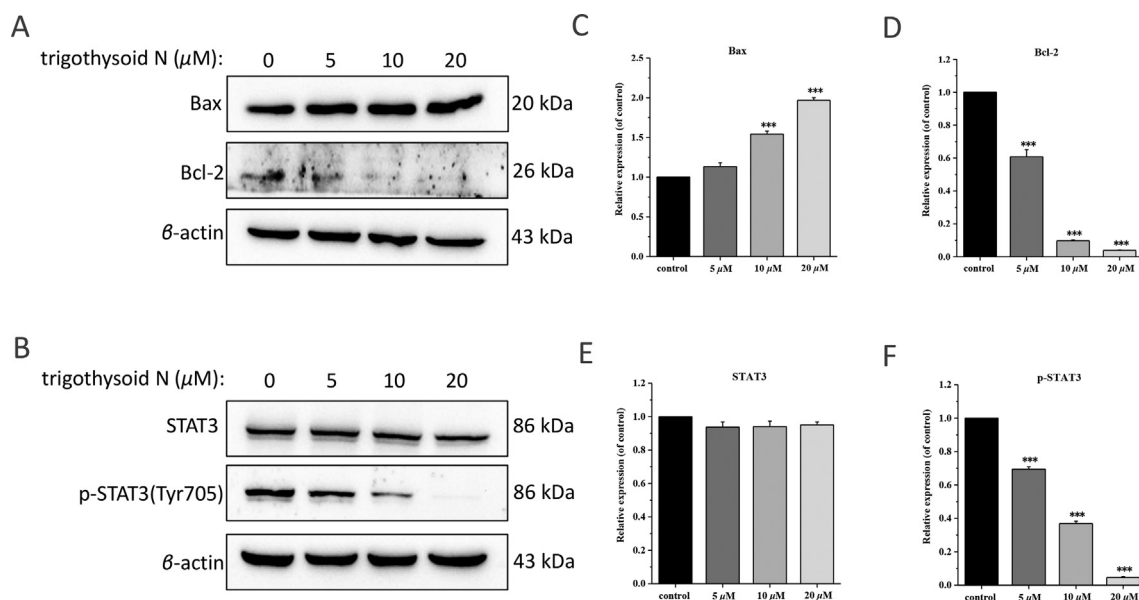


**Fig. 5** Effects of trigothyroid N on the expression of apoptosis-related proteins in A549 cells. A549 cells were pre-treated with trigothyroid N for 36 h, and western blotting analysis was performed. DMSO was used as a negative control. (A and B) The expression of Bax, Bcl-2, STAT3, p-STAT3. (C – F) Histogram of the protein relative expression level compared with control group.  $\beta$ -Actin protein was used as internal reference. n = 3, \* $P$  < 0.05, \*\*\* $P$  < 0.001 compared with control group cells. Data were obtained by at least three independent experiments.

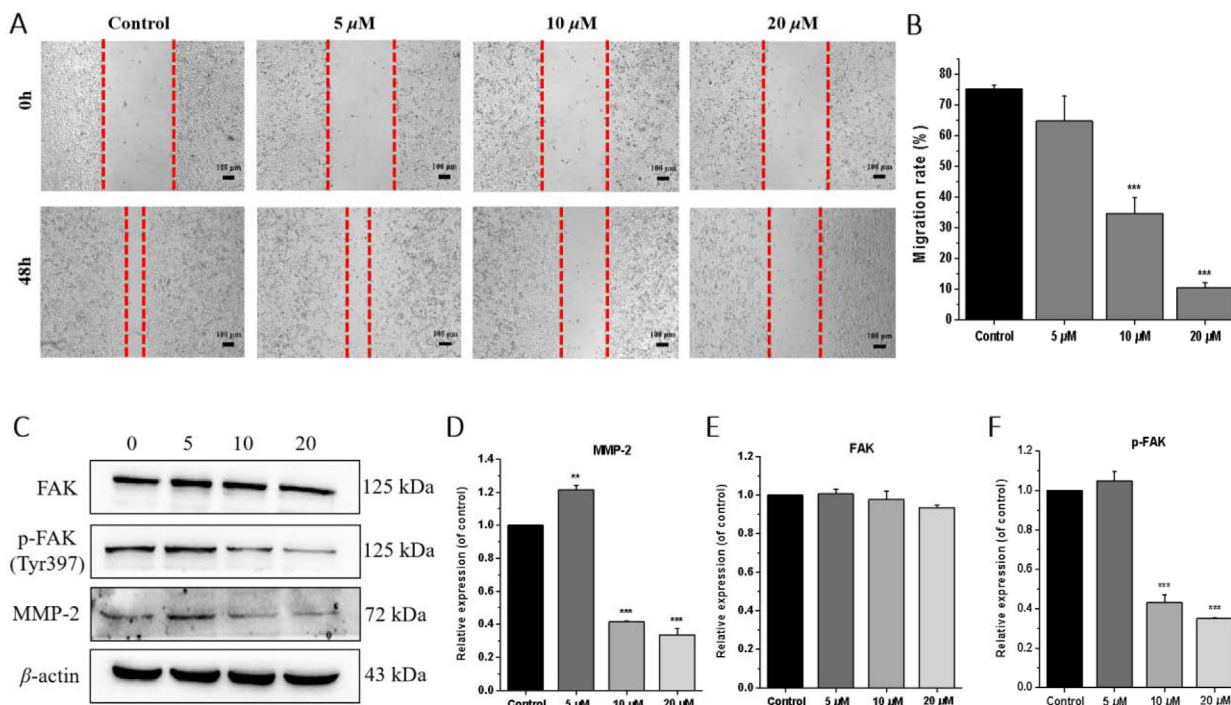


**Fig. 6** Trigothyroid N inhibited A549 cells migration via FAK signal pathway. (A) A549 cells were photographed at 0 h and 48 h (scale bar: 100 μm). Data of migration rate (%) were shown in B. (C) Western blotting results of metastasis-related protein levels. (D – F) Quantitative analysis of metastasis-related proteins expression.  $\beta$ -Actin protein was used as internal reference. DMSO was used as a negative control. n = 3, \*\* $P$  < 0.01, \*\*\* $P$  < 0.001 compared with control group cells. Data were obtained from at least three independent experiments.

with the control group, the fluorescence intensity of zebrafish embryos treated with trigothyroid N was reduced, and the fluorescence area migrated away from the primary sites decreased

significantly. After quantitative comparison (Fig. 8), the inhibitory rates of trigothyroid N on tumor cell proliferation were 5.7% (0.025 μM), 14.8% (0.05 μM) and 56.9% (0.1 μM),

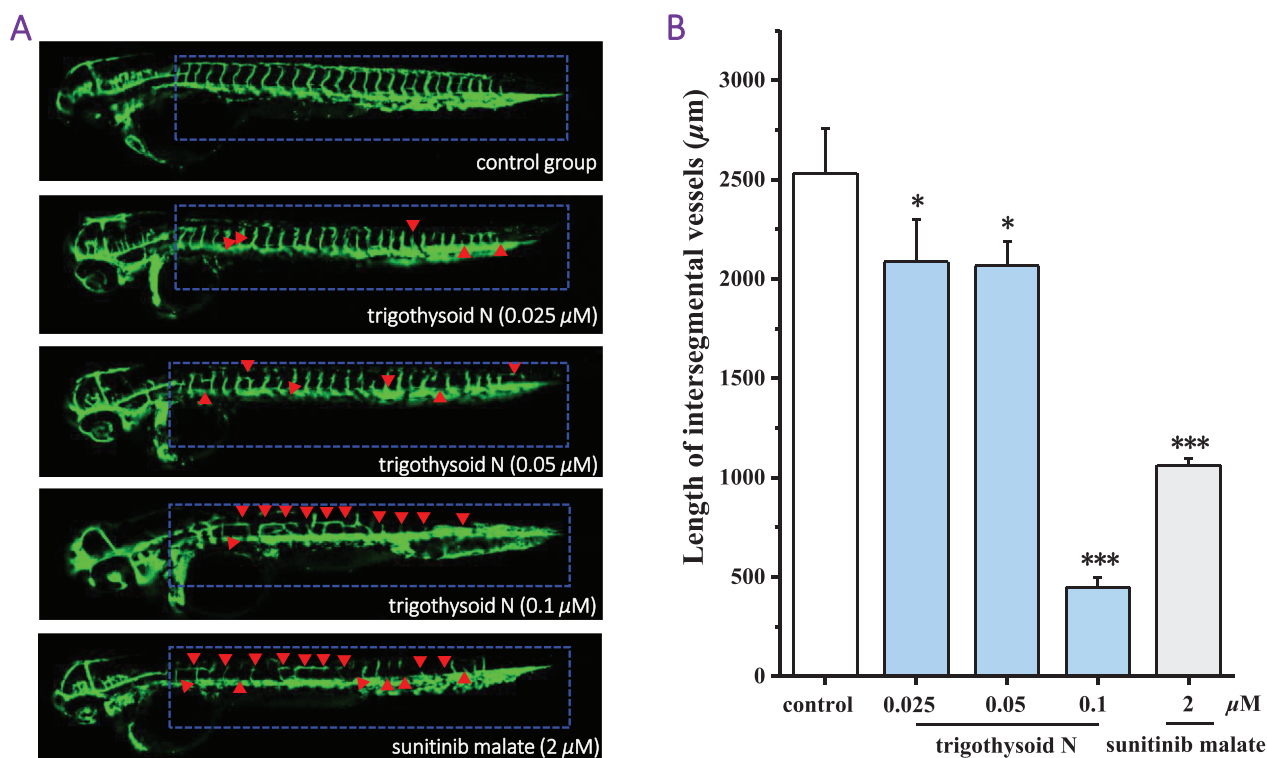


**Fig. 7** Anti-angiogenesis activity of trigothysoid N in the transgenic zebrafish model. The embryos from transgenic zebrafish *Tg (fli1:EGFP)* were treated with the tested compound and the anti-angiogenic compound, sunitinib malate (positive control). DMSO was used as a negative control. After exposure to the compounds for 48 h, the development of intersegmental blood vessels (ISVs) and dorsal longitudinal anastomotic vessels (DLAVs) were observed, and the length of ISVs was measured using ImageJ program. (A) Representative images of zebrafish embryos treated with vehicle, trigothysoid N and sunitinib malate. (B) The average length of ISVs of zebrafish after treating with different concentrations of trigothysoid N (0.025, 0.05, and 0.1 μM) ( $n = 15$  for each experimental group). \* $P < 0.5$ , \*\*\* $P < 0.001$  versus control group.

respectively. When the concentration reached 0.1 μM, the migration rate of tumor cells was inhibited by 30.8%, and the inhibitory activity was comparable to that of etoposide. These results revealed that trigothysoid N blocked tumor cell proliferation and migration *in vivo* to exert *in vivo* antitumor activity.

#### 4. Discussion

Under the background of the rising incidence rate of cancer, especially that of NSCLC, quite a few problems have emerged in clinical chemotherapy, such as adverse effects and drug resistance. The development of new drugs against NSCLC is urgent. For a long time, the great potential in disease treatment of phytochemicals has attracted much attention, prompting medicinal scientists to discover new anticancer lead compounds from natural products. In the current research, trigothysoid N, a diterpenoid obtained from *Trigonostemon thyrsoideus*, was found to have antiproliferative activity in the cellular assay, which showed the most inhibitory effects against A549 cells with an  $IC_{50}$  value of 6.4 μM.

The promising activity of cellular screening aroused our interest in the action mechanism of trigothysoid N. In the subsequent mechanistic studies conducted, trigothysoid N was found to arrest the cell cycle at G0/G1 phase for inhibiting

the proliferation of A549 cells. In addition to cell cycle arrest, MMP and ROS have been reported to be closely related to cell apoptosis. The experimental results discovered that trigothysoid N induced the loss of MMP and stimulated cellular ROS production to trigger ROS/MMP-dependent cell apoptosis (Shi et al., 2021). The expression changes of a series of proteins Bcl-2 and Bax occurred and verified trigothysoid N to spark the ROS/MMP-dependent cell apoptosis.

Accumulating studies have demonstrated that biologically activated STAT3 plays a crucial role in regulating various cellular events, such as cellular growth, survival, and apoptosis (Fathi et al., 2018; Thilakasiri et al., 2021). Yue et al. discovered azetidine-based small molecules inhibiting STAT3 activation and inducing antitumor response (Yue et al., 2022). Zhu et al. obtained the compound trichomicin from the fungus *Trichoderma harzianum*, which could effectively block the JAK-STAT3 signaling pathway mediated by IL-6 (Zhu et al., 2020). In the present study, Western blotting experiments showed that trigothysoid N can inactivate STAT3 by reducing the expression of p-STAT3. The detection of protein expression revealed that trigothysoid N regulated the STAT3 pathway to induce A549 cell apoptosis.

Migration is another significant characteristic of tumors, which has been reported to be closely associated with the occurrence and progression of tumors. The migration characteristic is another crucial reason that makes tumors difficult to

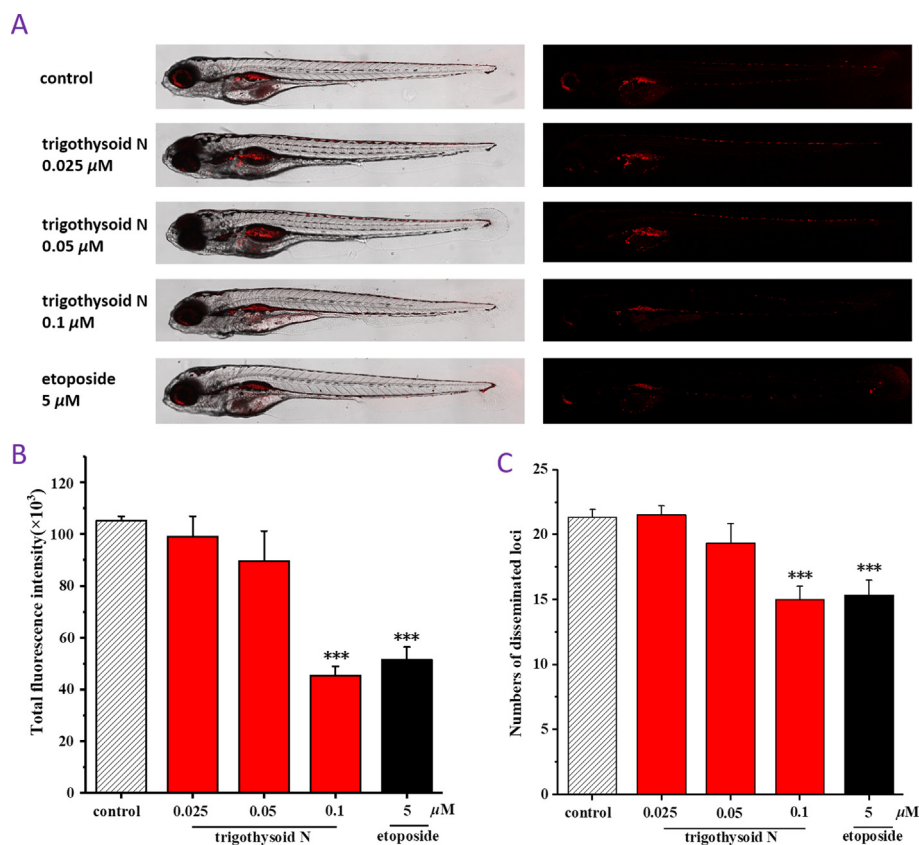


**Fig. 8** *In vivo* anti-tumor effects of trigothysoid N in zebrafish xenografts. CM-DiI-stained A549 cells were transplanted into 2 dpf zebrafish embryos by microinjecting. 4 h later, tumor-bearing embryos were treated with trigothysoid N (0.025, 0.05, and 0.1  $\mu$ M) and etoposide (5  $\mu$ M) for 48 h ( $n = 15$ /group). DMSO was used as a negative control. (A) Intensity and distribution of the red fluorescence were imaged under a confocal microscope. (B) Fluorescence intensity of the tumor xenografts, representing the number of A549 cells. (C) Quantification of the fluorescent area of the tumor xenografts, representing A549 cell metastasis. Results are expressed as mean  $\pm$  SD. \*\*\* $P < 0.001$  versus control group.

cure. Besides inhibiting tumor proliferation, the effects of trigothysoid N on tumor migration were also investigated. The wound-healing assay indicated that trigothysoid N inhibited A549 cell migration. Among numerous factors to affect tumor migration, FAK and the related pathway play a critical role (Paw et al., 2015; Qiu et al., 2022). As an essential intracellular tyrosine kinase, the expression and phosphorylation levels of FAK were elevated in invasive human cancers (Lee et al., 2015). FAK can induce integrin aggregation, thus promoting the expression of matrix metalloproteinase gene, and then up regulating the expression of matrix metalloproteinase-2 and matrix metalloproteinase-9 to promote cancer metastasis (Wu et al., 2021). In addition, it has been shown that the expression of matrix metalloproteinase-2 and matrix metalloproteinase-9 can be down-regulated by decreasing the phosphorylation levels of FAK, PI3K, AKT, and mTOR, thus inhibiting the migration and invasion of tumor cells. (Lin et al., 2014; Wu et al., 2020b). Our results demonstrated that trigothysoid N treatment inhibited the phosphorylation of FAK. Corresponding to the reduction of p-FAK, the downstream protein matrix metalloproteinase-2 was downregulated in the FAK-mediated signal pathway. According to these findings, trigothysoid N possessed antitumor activity through not only inhibiting tumor proliferation, but also blocking tumor migration.

In addition to the intrinsic characteristics of proliferation and migration, angiogenesis plays a crucial role in the development and progression of tumors, which can transport oxygen and nutrients (Chan et al., 2011). To inhibit tumor angiogenesis has become an important strategy for cancer treatment (Viallard and Larrivée, 2017; Li et al., 2019). In the present study, to investigate the effects of trigothysoid N on angiogenesis, a transgenic zebrafish model was established. As we expected, trigothysoid N showed anti-angiogenetic activity. It was found that the length of ISVs was significantly reduced after treatment with trigothysoid N. In particular, at the concentration of 0.1  $\mu$ M, the inhibitory activity on zebrafish angiogenesis of trigothysoid N was better than that of the positive drug sunitinib malate. According to the angiogenetic results, it was concluded that the antitumor effects of trigothysoid N were related to the inhibition of angiogenesis.

After revealing the possible antitumor mechanism of trigothysoid N, the *in vivo* antitumor activity using zebrafish xenografts was further conducted to explore the possible application as an antitumor agent against NSCLC. The zebrafish tumor model for the antitumor evaluation has many advantages, such as low drug dosage and easy detection, and has become an ideal *in vivo* screening model (Petrović et al., 2020). By microinjecting A549 cells into zebrafish embryos, the tumor model was constructed, and the *in vivo* antitumor

activity of trigothyoid N was evaluated. As expected, trigothyoid N showed dose-dependent inhibitory effects on tumor proliferation and metastasis in the zebrafish xenograft tumor model, which suggested that trigothyoid N may be considered as a lead molecule for NSCLC.

## 5. Conclusions

The side effects and drug resistance of chemotherapeutics make the development of new drugs for NSCLC to be urgent. Natural products have attracted extensive attention because of their structural and biological activity diversity, which are one of the sources of new drugs. Trigothyoid N, a natural diterpenoid, displayed significant anti-proliferation effects towards A549 cells. Besides cell cycle arrest and ROS increase, trigothyoid N also regulated the STAT3 and FAK signal pathways. For the possible antitumor application for NSCLC, trigothyoid N was examined the *in vivo* antitumor effects using the zebrafish tumor xenograft model and transgenic zebrafish model. Although the activity evaluation and preliminary mechanism research of trigothyoid N were completed, there is still a lot of work to be performed to promote the antitumor application for NSCLC.

## Authors' contributions

Ying Li performed cell experiments and zebrafish experiments and wrote the manuscript. Feng Liu obtained and identified the natural product. Yuhui Liu, Yeling Li and Yinan Zhao performed cell assays and revised the draft. Jing Xu and Yuanqiang Guo conceived, designed, and supervised the study and revised the manuscript. All authors read and approved the final manuscript.

## Declaration of Competing Interest

The authors declare that they have no known competing financial interests or personal relationships that could have appeared to influence the work reported in this paper.

## Acknowledgments

This research was supported financially by the National Natural Science Foundation of China (Nos. 22077067 and 22177054), Key Laboratory of Tropical Medicinal Resource Chemistry of Ministry of Education, Hainan Normal University (RDZH2021004), and the 111 Project B20016.

## Appendix A. Supplementary material

Supplementary data to this article can be found online at <https://doi.org/10.1016/j.arabjc.2023.104930>.

## References

- Bao, J., Zhao, Y., Xu, J., Guo, Y., 2021. Design and construction of IR780- and EGCG-based and mitochondrial targeting nanoparticles and their application in tumor chemo-phototherapy. *J. Mater. Chem. B* 9, 9932–9945.
- Chan, J.Y., Koon, J.C., Liu, X., Detmar, M., Yu, B., Kong, S.K., Fung, K.P., 2011. Polyphyllin D, a steroidal saponin from *Paris polyphylla*, inhibits endothelial cell functions *in vitro* and angiogenesis in zebrafish embryos *in vivo*. *J. Ethnopharmacol.* 137, 64–69.
- Chen, H., Zhou, B., Yang, J., Ma, X., Deng, S., Huang, Y., Wen, Y., Yuan, J., Yang, X., 2018. Essential oil derived from *Eupatorium adenophorum* spreng. mediates anticancer effect by inhibiting STAT3 and AKT activation to induce apoptosis in hepatocellular carcinoma. *Front. Pharmacol.* 9, 483.
- Cheng, Y.Y., Chen, H., He, H.P., Zhang, Y., Li, S.F., Tang, G.H., Guo, L.L., Yang, W., Zhu, F., Zheng, Y.T., Li, S.L., Hao, X.J., 2013. Anti-HIV active daphnane diterpenoids from *Trigonostemon thyrsoides*. *Phytochemistry* 96, 360–369.
- Courdavault, V., O'Connor, S.E., Oudin, A., Besseau, S., Papon, N., 2020. Towards the microbial production of plant derived anticancer drugs. *Trends in Cancer* 6, 444–448.
- Dai, R., Liu, M., Nik Nabil, W.N., Xi, Z., Xu, H., 2021. Mycomedicine: A unique class of natural products with potent anti-tumour bioactivities. *Molecules* 26, 1113.
- Fan, Z., Xu, Q., Wang, C., Lin, X., Zhang, Q., Wu, N., 2020. A tropomyosin-like *Meretrix meretrix* Linnaeus polypeptide inhibits the proliferation and metastasis of glioma cells via microtubule polymerization and FAK/Akt/MMPs signaling. *Int. J. Biol. Macromol.* 145, 154–164.
- Fathi, N., Rashidi, G., Khodadadi, A., Shahi, S., Sharifi, S., 2018. STAT3 and apoptosis challenges in cancer. *Int. J. Biol. Macromol.* 117, 993–1001.
- Ferlay, J., Colombet, M., Soerjomataram, I., Parkin, D.M., Piñeros, M., Znaor, A., Bray, F., 2021. Cancer statistics for the year 2020: An overview. *Int. J. Cancer.* 149, 778–789.
- Kim, D.H., Park, K.W., Chae, I.G., Kundu, J., Kim, E.H., Kundu, J. K., Chun, K.S., 2016. Carnosic acid inhibits STAT3 signaling and induces apoptosis through generation of ROS in human colon cancer HCT116 cells. *Mol. Carcinog.* 55, 1096–1110.
- Lee, B.Y., Timson, P., Horvath, L.G., Daly, R.J., 2015. FAK signaling in human cancer as a target for therapeutics. *Pharmacol. Ther.* 146, 132–149.
- Li, Y., Ma, J., Song, Z., Zhao, Y., Zhang, H., Li, Y., Xu, J., Guo, Y., 2021. The antitumor activity and mechanism of a natural diterpenoid from *Casearia graveolens*. *Front. Oncol.* 11, 688195.
- Li, S., Xu, H.X., Wu, C.T., Wang, W.Q., Jin, W., Gao, H.L., Li, H., Zhang, S.R., Xu, J.Z., Qi, Z.H., Ni, Q.X., Yu, X.J., Liu, L., 2019. Angiogenesis in pancreatic cancer: current research status and clinical implications. *Angiogenesis* 22, 15–36.
- Li, H.Y., Zhang, J., Sun, L.L., Li, B.H., Gao, H.L., Xie, T., Zhang, N., Ye, Z.M., 2015. Celastrol induces apoptosis and autophagy via the ROS/JNK signaling pathway in human osteosarcoma cells: an *in vitro* and *in vivo* study. *Cell Death Dis.* 6, 1604.
- Liang, Y., Zhang, Q., Yang, X., Li, Y., Zhang, X., Li, Y., Du, Q., Jin, D.Q., Cui, J., Lall, N., Tuerhong, M., Lee, D., Abudukeremu, M., Xu, J., Shuai, L., Guo, Y., 2020. Diterpenoids from the leaves of *Casearia kurzii* showing cytotoxic activities. *Bioorg. Chem.* 98, 103741.
- Lin, J.J., Su, J.H., Tsai, C.C., Chen, Y.J., Liao, M.H., Wu, Y.J., 2014. 11-*epi*-Sinulariolide acetate reduces cell migration and invasion of human hepatocellular carcinoma by reducing the activation of ERK1/2, p38MAPK and FAK/PI3K/AKT/mTOR signaling pathways. *Mar. Drugs* 12, 4783–4798.
- Lin, R., Sun, R., Xiao, T., Pei, S., Zhang, Q., Cheng, Y., Guo, X., Yang, Z., Gu, X., Zhang, F., Xie, C., Yang, C., 2022. Phenylpropenol ester and sesquiterpenoids with antimetastatic activities from the whole plants of *Chloranthus japonicus*. *Arab. J. Chem.* 15, 104100.
- Liu, F., Yang, X., Ma, J., Yang, Y., Xie, C., Tuerhong, M., Jin, D.Q., Xu, J., Lee, D., Ohizumi, Y., Guo, Y., 2017. Nitric oxide inhibitory daphnane diterpenoids as potential antineuroinflammatory agents for AD from the twigs of *Trigonostemon thyrsoides*. *Bioorg. Chem.* 75, 149–156.
- Liu, F., Yang, X., Liang, Y., Dong, B., Su, G., Tuerhong, M., Jin, D. Q., Xu, J., Guo, Y., 2018. Daphnane diterpenoids with nitric oxide inhibitory activities and interactions with iNOS from the leaves of *Trigonostemon thyrsoides*. *Phytochemistry* 147, 57–67.

- Paw, I., Carpenter, R.C., Watabe, K., Debinski, W., Lo, H.W., 2015. Mechanisms regulating glioma invasion. *Cancer Lett.* 362, 1–7.
- Petrović, J., Glamočlija, J., Ilić-Tomić, T., Soković, M., Robajac, D., Nedić, O., Pavić, A., 2020. Lectin from *Laetiporus sulphureus* effectively inhibits angiogenesis and tumor development in the zebrafish xenograft models of colorectal carcinoma and melanoma. *Int. J. Biol. Macromol.* 148, 129–139.
- Qiu, Y., Fang, B., Thuy, N.T.T., Li, A., Yoo, H.M., Zheng, X., Cho, N., 2022. Narciclasine suppresses esophageal cancer cell proliferation and migration by inhibiting the FAK signaling pathway. *Eur. J. Pharmacol.* 921, 174669.
- Rocha-Brito, K.J.P., Fonseca, E.M.B., de Freitas Oliveira, B.G., de Fátima, Á., Ferreira-Halder, C.V., 2020. Calix [6] arene diminishes receptor tyrosine kinase lifespan in pancreatic cancer cells and inhibits their migration and invasion efficiency. *Bioorg. Chem.* 100, 103881.
- Shi, L., Gao, L.L., Cai, S.Z., Xiong, Q.W., Ma, Z.R., 2021. A novel selective mitochondrial-targeted curcumin analog with remarkable cytotoxicity in glioma cells. *Eur. J. Med. Chem.* 221, 113528.
- Shi, L., Li, Y., Zhang, S., Gong, X., Xu, J., Guo, Y., 2022. Construction of inulin-based selenium nanoparticles to improve the antitumor activity of an inulin-type fructan from chicory. *Int. J. Biol. Macromol.* 210, 261–270.
- Sung, H., Ferlay, J., Siegel, R.L., Laversanne, M., Soerjomataram, I., Jemal, A., Bray, F., 2021. Global cancer statistics 2020: GLOBOCAN estimates of incidence and mortality worldwide for 36 cancers in 185 countries. *CA Cancer J. Clin.* 71, 209–249.
- Thilakasiri, P.S., Dmello, R.S., Nero, T.L., Parker, M.W., Ernst, M., Chand, A.L., 2021. Repurposing of drugs as STAT3 inhibitors for cancer therapy. *Semin. Cancer Biol.* 68, 31–46.
- Viallard, C., Larrivé, B., 2017. Tumor angiogenesis and vascular normalization: alternative therapeutic targets. *Angiogenesis* 20, 409–426.
- Wang, H., Li, Y., Wang, X., Li, Y., Cui, J., Jin, D.Q., Tuerhong, M., Abudukeremu, M., Xu, J., Guo, Y., 2022a. Preparation and structural properties of selenium modified heteropolysaccharide from the fruits of *Akebia quinata* and *in vitro* and *in vivo* antitumor activity. *Carbohydr. Polym.* 278, 118950.
- Wang, X., Li, N., Li, Y., Zhao, Y., Zhang, L., Sun, Y., Ohizumi, Y., Xu, J., Guo, Y., 2022b. A novel polysaccharide from *Paonia lactiflora* exerts anti-tumor activity via immunoregulation. *Arab. J. Chem.* 15, 104132.
- Wang, H., Lin, Z., Li, Y., Wang, X., Xu, J., Guo, Y., 2023. Characterization, selenylation, and antineoplastic effects on HepG2 cells *in vitro* and *in vivo* of an arabinofuranan from the fruits of *Akebia quinata*. *Arab. J. Chem.* 16, 104448.
- Wu, S.J., Arundhati, A., Wang, H.C., Chen, C.Y., Cheng, T.M., Yuan, S.F., Wang, Y.M., 2021. Migration and invasion of NSCLC suppressed by the downregulation of Src/focal adhesion kinase using single, double and tetra domain anti-CEACAM6 antibodies. *Transl. Oncol.* 14, 101057.
- Wu, P., Song, Z., Li, Y., Wang, H., Zhang, H., Bao, J., Li, Y., Cui, J., Jin, D.Q., Wang, A., Liang, B., Lee, D., Xu, J., Guo, Y., 2020a. Natural iridoids from *Patrinia heterophylla* showing anti-inflammatory activities *in vitro* and *in vivo*. *Bioorg. Chem.* 104, 104331.
- Wu, Y.J., Wei, W.C., Dai, G.F., Su, J.H., Tseng, Y.H., Tsai, T.C., 2020b. Exploring the mechanism of flaccidoxide-13-acetate in suppressing cell metastasis of hepatocellular carcinoma. *Mar. Drugs* 18, 314.
- Yao, M., Li, R., Yang, Z., Ding, Y., Zhang, W., Li, W., Liu, M., Zhao, C., Wang, Y., Tang, H., Wang, J., Wen, A., 2020. PP9, a steroidal saponin, induces G2/M arrest and apoptosis in human colorectal cancer cells by inhibiting the PI3K/Akt/GSK3 $\beta$  pathway. *Chem-Biol. Interact.* 331, 109246.
- Ye, Y., Zhang, T., Yuan, H., Li, D., Lou, H., Fan, P., 2017. Mitochondria-targeted lupane triterpenoid derivatives and their selective apoptosis-inducing anticancer mechanisms. *J. Med. Chem.* 60, 6353–6363.
- Ye, T., Zhu, S., Zhu, Y., Feng, Q., He, B., Xiong, Y., Zhao, L., Zhang, Y., Yu, L., Yang, L., 2016. Cryptotanshinone induces melanoma cancer cells apoptosis via ROS-mitochondrial apoptotic pathway and impairs cell migration and invasion. *Biomed. Pharmacother.* 82, 319–326.
- Yin, W.M., Cao, X.B., Li, S.X., Zhang, F., Guan, Y.F., 2022. Brassinin inhibits proliferation and induces cell cycle arrest and apoptosis in nasopharyngeal cancer C666-1 cells. *Arab. J. Chem.* 15, 104018.
- Yu, Y., Sun, F., Zhang, C., Wang, Z., Liu, J., Tan, H., 2016. Study on glyco-modification of endostatin-derived synthetic peptide endostatin2 (ES2) by soluble chitooligosaccharide. *Carbohydr. Polym.* 154, 204–213.
- Yue, P., Zhu, Y., Brotherton-Pleiss, C., Fu, W., Verma, N., Chen, J., Nakamura, K., Chen, W., Chen, Y., Alonso-Valenteen, F., Mikhael, S., Medina-Kauwe, L., Kershaw, K.M., Celeridad, M., Pan, S., Limpert, A.S., Sheffler, D.J., Cosford, N.D.P., Shiao, S.L., Tius, M.A., Lopez-Tapia, F., Turkson, J., 2022. Novel potent azetidone-based compounds irreversibly inhibit Stat3 activation and induce antitumor response against human breast tumor growth *in vivo*. *Cancer Lett.* 534, 215613.
- Zhang, C., Liu, K., Yao, K., Reddy, K., Zhang, Y., Fu, Y., Yang, G., Zykova, T.A., Shin, S.H., Li, H., Ryu, J., Jiang, Y.N., Yin, X., Ma, W., Bode, A.M., Dong, Z., Dong, Z., 2015. HOI-02 induces apoptosis and G2-M arrest in esophageal cancer mediated by ROS. *Cell Death Dis.* 6, 1912.
- Zhang, J., Song, Z., Li, Y., Zhang, S., Bao, J., Wang, H., Dong, C., Ohizumi, Y., Xu, J., Guo, Y., 2021a. Structural analysis and biological effects of a neutral polysaccharide from the fruits of *Rosa laevigata*. *Carbohydr. Polym.* 265, 118080.
- Zhang, X., Song, Z., Li, Y., Wang, H., Zhang, S., Reid, A.M., Lall, N., Zhang, J., Wang, C., Lee, D., Ohizumi, Y., Xu, J., Guo, Y., 2021c. Cytotoxic and antiangiogenic xanthenes inhibiting tumor proliferation and metastasis from *Garcinia xipshuanbannaensis*. *J. Nat. Prod.* 84, 1515–1523.
- Zhang, S., Zhang, H., Shi, L., Li, Y., Tuerhong, M., Abudukeremu, M., Cui, J., Li, Y., Jin, D.Q., Xu, J., Guo, Y., 2021b. Structure features, selenylation modification, and improved anti-tumor activity of a polysaccharide from *Eriobotrya japonica*. *Carbohydr. Polym.* 273, 118496.
- Zhao, Y., Zhang, X., Li, Y., Li, Y., Zhang, H., Song, Z., Xu, J., Guo, Y., 2022. A natural xanthone suppresses lung cancer growth and metastasis by targeting STAT3 and FAK signaling pathways. *Phytomedicine* 102, 154118.
- Zhou, L., Song, Z., Zhang, S., Li, Y., Xu, J., Guo, Y., 2021. Construction and antitumor activity of selenium nanoparticles decorated with the polysaccharide extracted from *Citrus limon* (L.) Burm. f. (Rutaceae). *Int. J. Biol. Macromol.* 188, 904–913.
- Zhou, L., Li, Y., Gong, X., Li, Z., Wang, H., Ma, L., Tuerhong, M., Abudukeremu, M., Ohizumi, Y., Xu, J., Guo, Y., 2022. Preparation, characterization, and antitumor activity of *Chaenomeles speciosa* polysaccharide-based selenium nanoparticles. *Arab. J. Chem.* 15, 103943.
- Zhu, F., Zhao, X., Li, J., Guo, L., Bai, L., Qi, X., 2020. A new compound Trichomicin exerts antitumor activity through STAT3 signaling inhibition. *Biomed. Pharmacother.* 121, 109608.